Iterative Detection and Decoding (IDD) MIMO-OFDM HARQ Algorithm with Antenna Scheduling

KyooHyun Kim, SeungWon Kang, Manar Mohaisen, and KyungHi Chang

The Graduate School of IT & Telecommunications, InHa University

Incheon, Korea

E-mail: makewish79@paran.com, swkang79@hanmail.net, lemanar@hotmail.com, khchang@inha.ac.kr

Abstract In this paper, a multiple-input-multiple-output (MIMO) hybrid-automatic repeat request (HARQ) algorithm based on antenna scheduling is proposed. It retransmits the packet using the scheduled antennas according to the state of the communication link, instead of retransmitting the packet through the same antennas. The proposed MIMO-OFDM HARQ system based on antenna scheduling is shown to be superior to conventional MIMO HARQ systems due to its spatial diversity gain.

Key words: *MIMO-OFDM, I-BLAST, Sphere Decoding, Chase Combining, Incremental Redundancy, Antenna Scheduling.*

1. Introduction

MIMO systems that employ several transmit and receive antennas at both ends are capable of providing a large increase in capacity compared to traditional single antenna systems. However, MIMO systems suffer from co-antenna interference (CAI) and frequency-selective fading. CAI, one of the major drawbacks in MIMO systems, can be mitigated by employing an iterative detection and decoding (IDD) type of receiver. The basic idea of IDD is the exchange of information between the detector and the decoder in an iterative fashion, until the performance no longer can be improved [1]. The robustness on frequency-selective fading can be improved by combining OFDM with MIMO techniques [2]-[3].

Many modern data communication systems make use of HARQ schemes, which combine forward error correction (FEC) and ARQ protocols. There are many variants of HARQ schemes. Among them, chase combining (CC) and incremental redundancy (IR) are the most usual applications. When the original transmission fails, CC re-sends the same copy again to be combined with what sent in the original transmission, while IR re-sends the packets by applying lower code rate and combines those with original transmitted packets [4]-[5]. For a conventional MIMO HARQ system, if the channel status of the communication link for the antenna continues to operate under bad conditions, the retransmitted packets can also be erroneous, which would increase the number of retransmissions, causing the system to function poorly. Therefore, in this paper, a modified MIMO HARQ algorithm incorporated with antenna scheduling is proposed to solve the problem mentioned above. Furthermore, to increase the data rate and to improve the performance further, the IDD-based Bell laboratory layered space-time (I-BLAST) system is utilized with the proposed MIMO HARQ algorithm.

This paper is organized as follows: In Sect. 2, the I-BLAST system and sphere decoding (SD) algorithm are briefly described. In Sect. 3, the details of the I-BLAST system with the proposed HARQ algorithm with antenna scheduling is described. In Sect. 4, the performance of the I-BLAST system and the proposed HARQ algorithm is evaluated by computer simulation, and finally in Sect. 5, the conclusions are given.

2. I- BLAST System

The major factor degrading the performance of the BLAST system is the aforementioned CAI, which is caused by transmitting the signal using n_T antennas. This issue, however, can be cancelled applying an IDD receiver, creating what has been termed the I-BLAST system.

2.1 Transmitter of I-BLAST System

Figure 1 shows the transmitter architecture of the I-BLAST system with n_T transmitting antennas, including the conventional V-BLAST (Vertical BLAST) system with a diagonal space (DS) interleaver. The input bit sequence **b** is de-multiplexed and encoded by an error-correcting code to generate the coded bit sequence **c**, which is further interleaved by a diagonal space bit interleaver to obtain the interleaved coded bit sequence $\tilde{\mathbf{c}}$.

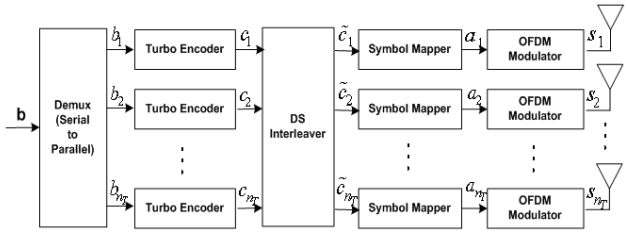

Fig. 1 Transmitter architecture of the I-BLAST system.

1	4	3	2	1	4	3	2	1
2	1	4	3	2	1	4	3	2
3	2	1	4	3	2	1	4	3
4	3	2	1	4	3	2	1	4

Fig. 2 Diagonal space interleaver.

Figure 2 shows the diagonal space interleaver based on the diagonal layering of each independently coded substream. It is interesting to note that unlike D-BLAST (Diagonal BLAST), no boundary wastage occurs [5]. The interleaved sequence $\tilde{\mathbf{c}}$ has q coded bits in each transmitting antenna branch to be mapped by M-QAM, so the total $q \cdot n_T$ coded bits are in $\boldsymbol{a}$, where $q = \log_2 M$. The $n_T -$ dimensional signal vector $a = [a_1, a_2, \ldots, a_{n_T}]^T$ is forwarded to the OFDM modulator, which performs an inverse fast Fourier transform (IFFT) followed by a virtual carrier / guard interval (GI) insertion. It is then transmitted through n_T antennas.

2.2 Receiver of I-BLAST System

Figure 3 shows the architecture of the iterative receiver used in I-BLAST. The main components of the receiver are the inner soft-input soft-output (SISO) decoder, the DS (de-) interleaver and the n_R parallel outer SISO decoder.

Assuming an $n_T \times 1$ OFDM symbol vector $\mathbf{s}$ is transmitted over an n_R x n_T MIMO channel $\mathbf{H}$, the n_R x 1 received signal vector $\mathbf{r}$ can be expressed by Eq. (1).

$$\mathbf{r}^{(k)} = \mathbf{H}\mathbf{s}^{(k)} + \mathbf{n}^{(k)} \tag{1}$$

In Eq. (1), k is the symbol index and $\mathbf{n}$ is the $n_R \times 1$ additive white Gaussian noise with a zero mean and variance $\sigma^2 \mathbf{I}_{n_R}$.

The LLR (Log Likelihood Ratio) of the interleaved bit sequence $\tilde{\mathbf{c}} = [\tilde{c}_1, \tilde{c}_2, \ldots, \tilde{c}_{q \cdot n_T}]^T$ is defined then by Eq. (2) [1], [6].

$$L(\tilde{c}_i) = \log \frac{\Pr[\tilde{c}_i = 1 \mid \mathbf{r}]}{\Pr[\tilde{c}_i = 0 \mid \mathbf{r}]}, \quad i = 1, 2, \ldots, q \cdot n_T$$

using Bay's rule,

$$= \log \frac{\Pr[\mathbf{r} \mid \tilde{c}_i = 1] \Pr[\tilde{c}_i = 1]}{\Pr[\mathbf{r} \mid \tilde{c}_i = 0] \Pr[\tilde{c}_i = 0]} \tag{2}$$

$$= \log \frac{\sum_{\mathbf{s} \in S_i^1} \exp(-\frac{1}{2\sigma^2} \|\mathbf{r} - \mathbf{H}\mathbf{s}\|^2) \Pr[\mathbf{s}]}{\sum_{\mathbf{s} \in S_i^0} \exp(-\frac{1}{2\sigma^2} \|\mathbf{r} - \mathbf{H}\mathbf{s}\|^2) \Pr[\mathbf{s}]}$$

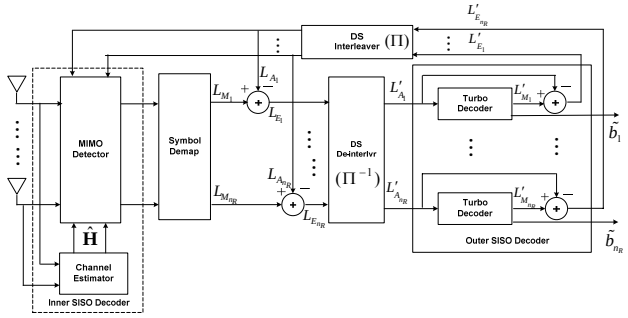

Fig. 3 Receiver architecture of the I-BLAST system.

In Eq. (2), $\Pr[\tilde{c}_i = b]$, where b has a value of 0 or 1, is the intrinsic information of the coded bit $\tilde{c}_i$, and S_i^c is written as Eq. (3).

$$S_i^c = \{\mu(\tilde{\mathbf{c}}) \mid \tilde{\mathbf{c}} = [\tilde{c}_1, \tilde{c}_2, \ldots, \tilde{c}_{q \cdot n_T}], \tilde{c} = c\} \tag{3}$$

Here, $\mu(\cdot)$ denotes a modulation function. During the first iteration, the initial intrinsic probabilities of all symbol bits are assumed to be 1/2 (i.e., equally likely). Using the approximate expression of $\sum P_i \simeq \max\{P_i\}$, Eq. (2) is rewritten as Eq. (4) [6].

$$\begin{aligned} L(\tilde{c}_i) \cong & \frac{1}{2\sigma^2} [\min_{\mathbf{s} \in S_i^1} \{\|\mathbf{r} - \mathbf{H}\mathbf{s}\|^2 - \log \Pr[\mathbf{s}]\}] \\ & - \frac{1}{2\sigma^2} [\min_{\mathbf{s} \in S_i^0} \{\|\mathbf{r} - \mathbf{H}\mathbf{s}\|^2 - \log \Pr[\mathbf{s}]\}] \end{aligned} \tag{4}$$

A-priori LLR value $L_E(\tilde{c}_i)$ obtained by Eq. (4) is de-interleaved and used for the outer SISO decoder. $\tilde{c}_i$ in Eq. (4) becomes c_i after the DS de-interleaver (Π^{-1}) , and becomes $\tilde{c}_i$ again after the DS interleaver (Π) in the feedback path. The relationship of the LLRs $L'(c)$ and $L(\tilde{c})$ is given by Eq. (5).

$$\begin{aligned} L'(c) &= \Pi^{-1}\{L(\tilde{c})\} \\ L(\tilde{c}) &= \Pi\{L'(c)\} \end{aligned} \tag{5}$$

Based on the a-priori information $L'_A(c_i)$, the outer SISO decoder yields a-posteriori information $L'_M(c_i)$ as expressed by Eq. (6).

$$L'_M(c_i) = L'_A(c_i) + L'_E(c_i) \tag{6}$$

In above equation, $L'_E(c_i)$ is termed extrinsic information and is obtained through a decoding process. This value is interleaved and calculated for Eq. (7).

$$\Pr[\mathbf{s}] = \prod_{i=1}^{q \cdot n_T} \frac{[\exp\{L_E(\tilde{c}_i)\}]^{\tilde{c}_i}}{1 + \exp[L_E(\tilde{c}_i)]} \tag{7}$$

Eq. (7) is used as a-priori probability $L'_A(c_i)$ in Eq. (6) at the next iteration. As the number of iterations increases, the performance of the I-BLAST system is improved due to the more accurate a priori probability in Eq. (7) [6].

2.3 Detection for I-BLAST System

Maximum likelihood (ML) decoding over a multi-path channel requires an exhaustive search over all possible codewords. Thus, the computational complexity of the optimal decoding exponentially increases according to the length of the codeword.

An efficient ML detection technique has been proposed to lower the computational complexity without sacrificing the performance compared to the case of the optimal ML, which is known as the sphere decoding (SD) algorithm [7]. The principle of the sphere decoding algorithm is to find the closest lattice point to the received signal within a sphere radius where each codeword is represented by a lattice point in a constellation coordinator. To employ the sphere decoding algorithm, the notation of Eq. (1) is changed to Eq. (8).

$$\mathbf{r}' = \mathbf{M}\mathbf{s}' + \mathbf{n}' \tag{8}$$

Here, $\mathbf{r}'$, $\mathbf{M}$, $\mathbf{s}'$ and $\mathbf{n}'$ are real values of the received signal, channel matrix, transmitted signal, and noise vector, respectively.

$$\begin{aligned}
\mathbf{r}' &= [\mathrm{Re}\{\mathbf{r}\} \quad \mathrm{Im}\{\mathbf{r}\}]^T \\
\mathbf{M} &= \begin{bmatrix} \mathrm{Re}\{\mathbf{H}\} & -\mathrm{Im}\{\mathbf{H}\} \\ \mathrm{Im}\{\mathbf{H}\} & \mathrm{Re}\{\mathbf{H}\} \end{bmatrix} \\
\mathbf{s}' &= [\mathrm{Re}\{\mathbf{s}\} \quad \mathrm{Im}\{\mathbf{s}\}]^T \\
\mathbf{n}' &= [\mathrm{Re}\{\mathbf{n}\} \quad \mathrm{Im}\{\mathbf{n}\}]^T
\end{aligned} \tag{9}$$

In Eq. (9), $\mathrm{Re}\{\cdot\}$ and $\mathrm{Im}\{\cdot\}$ represent the real and imaginary part of a complex signal, respectively. Each symbol s'_i in the vector $\mathbf{s}'$ is referred to as a layer; each is constrained to a finite set μ in Eq. (10).

$$\begin{aligned}
&\text{QPSK}: \ \mu \in \{-1, +1\} \\
&\text{16QAM}: \ \mu \in \{-3, -1, +1, +3\} \\
&\text{64QAM}: \ \mu \in \{-7, -5, -3, -1, +1, +3, +5, +7\}
\end{aligned} \tag{10}$$

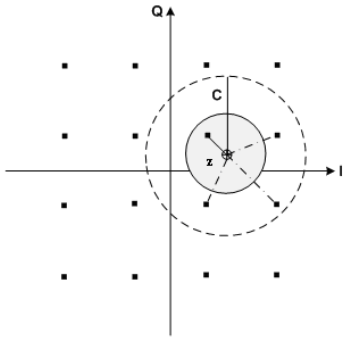

Fig. 4 Geometrical representation of the sphere decoding algorithm.

Description of the SD algorithm is illustrated in Fig. 4. Initially, Eq. (11) is defined to lead to the SD algorithm.

$$\mathbf{s}'_{SD} = \arg\min_{\mathbf{s}' \in \mu} (\mathbf{z} - \mathbf{s}')^T \mathbf{M}^T \mathbf{M} (\mathbf{z} - \mathbf{s}') \tag{11}$$

Here, $\mathbf{z} = (\mathbf{M}^T\mathbf{M})^{-1}\mathbf{M}^T\mathbf{r}'$ is a zero-forcing point. At each recursion, the SD stores in radius *C*, which is the best vector value previously found, where radius *C* is given as Eq. (12).

$$C = d(\mathbf{z}, \mathbf{s}'), \quad \text{where } d: \text{Euclidean Distance} \tag{12}$$

It is interesting to note that there is no need to continue and check vectors that can only be worse than this point; therefore, the search can be constrained to a sphere as Eq. (13) [8].

$$(\mathbf{z} - \mathbf{s}')^T \mathbf{M}^T \mathbf{M} (\mathbf{z} - \mathbf{s}') \le C \tag{13}$$

Using a factorization such as Cholesky or QR [9], the matrix $\mathbf{M}^T\mathbf{M}$ can be transformed into $\mathbf{R}^T\mathbf{R}$, where $\mathbf{R}$ is a $n_T \times n_T$ upper triangular matrix.

$$\mathbf{R} = \begin{pmatrix} R_{1,1} & \cdots & \mathrm{R}_{1,n_T} \\ & \ddots & \vdots \\ 0 & & \mathrm{R}_{n_T,n_T} \end{pmatrix} \tag{14}$$

Using Eq. (14), Eq. (13) can be rewritten as

$$\sum_{i=1}^{n_R}\left[\sum_{j=i}^{n_T} R_{ij}(\mathbf{z}-\mathbf{s}')\right]^2 \le C\ . \qquad (15)$$

3. MIMO HARQ Algorithm with Antenna Scheduling

Conventional MIMO HARQ algorithms retransmit packets using the same antennas when the transceiver receives the negative acknowledgement (NAK) on its feedback link. If the channel status of the communication link for the antenna remains in a poor condition, the retransmitted packet may continue to be erroneous, and the number of retransmissions would then increase continuously, leading to additional poor system performance.

In this section, a MIMO HARQ algorithm based on antenna scheduling is proposed. The proposed algorithm retransmits the packet using scheduled antennas according to the state of the communication link, as opposed to retransmitting the packet through the same antennas. A stop-and-wait (SAW) ARQ scheme is assumed, which transmits the next packet after receiving the ACK or NAK.

3.1 System Model

Figure 5 shows the I-BLAST transmitter architecture with the proposed MIMO HARQ algorithm with antenna scheduling. The main components of the transmitter are a cyclic redundancy check (CRC) encoder, conventional transmit blocks of I-BLAST, a transmit antenna selection block and a resource scheduler.

The CRC encoder generates a CRC code to check whether an error occurs in the CRC decoder. The Tx antenna selection block selects the L_T transmitting antenna branches, which has high channel-sum values in Eq. (17), among total n_T antennas. Utilizing feedback information, the resource scheduler controls the code rate of the turbo encoder and determines the antennas that will transmit the signal. In Fig. 5, $\{\Im_{T_n}, ACK\}$, $j = 1, 2, \ldots, n_T$ are the channel sum and ACK value, respectively.

Figure 6 (b) shows the receiver architecture of I-BLAST with the proposed MIMO HARQ algorithm with antenna scheduling. The main components of the receiver are the conventional receive blocks of I-BLAST, the receive antenna selection block and the CRC decoder. Estimated channel values are used to calculate the channel sum and to select the $L_R \times L_T$ antennas.

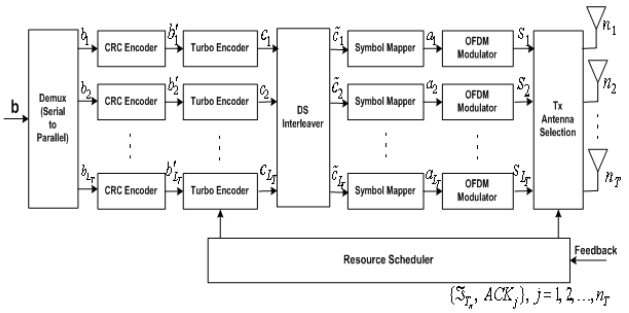

Fig. 5 Transmitter architecture of I-BLAST with the proposed HARQ algorithm with antenna scheduling.

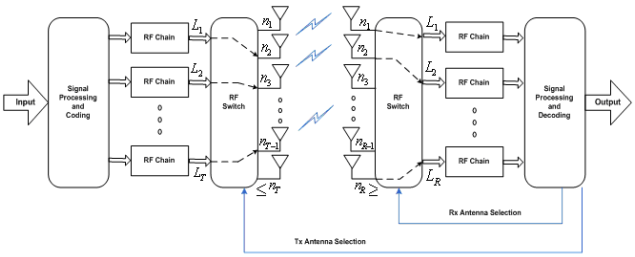

(a)

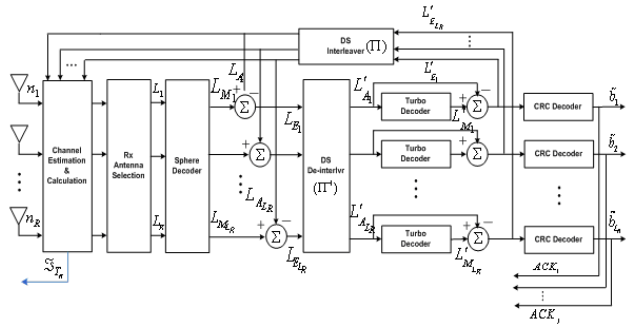

(b)

Fig. 6 (a) Joint Tx/Rx antenna selection block. (b) Receiver architecture of I-BLAST with the proposed HARQ algorithm with antenna scheduling.

A joint transmit / receive antenna selection algorithm is used to select the $L_R \times L_T$ antennas among $n_R \times n_T$ antennas. The CRC decoder extracts the CRC sequence from the turbo-decoded bit sequence and determines whether an error has occurred.

3.2 Proposed MIMO HARQ Algorithm with Antenna Scheduling

Figure 7 shows a flow chart of the proposed MIMO HARQ algorithm in the downlink.

Transmitter receives the feedback information of channel sum values and ACK values, as expressed by Eq. (16). It then determines the strategy of retransmission, as follows.

$$\{\Im_{T_n}, ACK_j\}, \quad j = 1,\ 2,\ \ldots,\ n_T \tag{16}$$

Initially, among n_T antennas L_T Tx antennas are selected according to the order of the channel sum values $\Im_{T_n}$ in Eq. (17). Also chosen are the antennas for retransmission according to the order of the channel sum values. The scheduler at the transmitter side then checks the ACK value of each antenna.

- If all Tx antennas receive the value of 1 (NAK), then an incremental redundancy scheme is employed to achieve robust packet retransmission over the communication link. In this case, all L_T antennas are utilized for the retransmission.
- If the number of ACKs is greater than or equal to the number of NAKs, the scheduler retransmits by applying chase combining using as many ACK antennas as the number of NAKs.
- If the number of NAKs is greater than the number of ACKs, the scheduler retransmits by applying chase combining using the ACK antennas, and by applying incremental redundancy using as many NAK antennas as in: (number of NAK antennas – number of ACK antennas).

On the receiver side, channel sum values are obtained by Eq. (17).

$$\begin{aligned} \Im_{T_n}^{Sum} &= \sum_{m=1}^{n_R} |H_{mn}|,\ n = 1,\ 2,\ \ldots,\ n_T \\ \Im_{R_m}^{Sum} &= \sum_{n=1}^{n_T} |H_{mn}|,\ m = 1,\ 2,\ \ldots,\ n_R \end{aligned} \tag{17}$$

After calculating the channel sum values, the Rx antenna selector selects L_R Rx antennas among n_R antennas, which are selected according to the order of the channel sum values $\Im_{R_m}$ in Eq. (17). The receiver then checks whether the received packet is a retransmitted packet.

For retransmitted packet reception, the receiver combines the retransmitted packet with the original received packet in the buffer, and CRC decoding is then performed. The determination of an error is examined using Eqs. (18) and (19). [10]

$$Error\ Check : \left[\frac{P(x)}{G(x)} = Q(x) + R(x) \right] \tag{18}$$

$$ACK = \begin{cases} 0: \text{ No Error} & \text{if } R(x) = 0 \\ 1: \text{ Error} & \text{if } R(x) \neq 0 \end{cases} \tag{19}$$

In Eq. (18), $P(x)$, $G(x)$, $Q(x)$, and $R(x)$ are the information polynomial, CRC polynomial, quota, and remainder, respectively. If the remainder $R(x)$ is zero, there are no transmission errors.

4. Simulation Results

In this section, the performance of I-BLAST is evaluated through computer simulation and an optimal iteration number for the IDD is determined. The performance of MIMO detection algorithms are compared with each other, and the performance of a conventional MIMO-HARQ algorithm is also compared with the proposed antenna scheduling-based MIMO-HARQ algorithm to show the gain due to the spatial diversity.

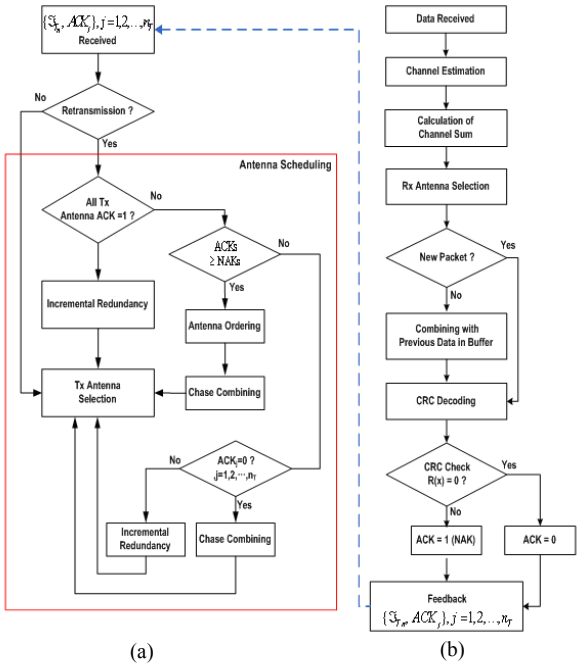

(a) (b)

Fig. 7 (a) The proposed MIMO HARQ algorithm at the downlink transmitter side. (b) The proposed MIMO HARQ algorithm at the downlink receiver side.

The MIMO channel model used for simulation is spatial channel model extension (SCM-E) of 3rd generation partnership project ad-hoc group (3GPP AHG) [11].The simulation parameters are summarized in Table 1. Figure 8 shows the structure of sub-frame construction and pilot assignment per antenna, which is being employed in 3GPP LTE (Long Term Evolution) standardization [12].

Table 1 Simulation parameters.

Parameters	***Value***
Carrier Frequency	2 GHz
Bandwidth of Operation	20 MHz
Number of FFT Points	2048
Cyclic Prefix	146
Modulation	QPSK, 16QAM
Sub-frame Duration	0.5 ms
OFDM Symbol per Sub-frame	7
Mobile Speed	120 km/h
MIMO Fading Channel Model	SCM-E Sub-urban Macro
Channel Estimation	Practical
MIMO Detection	ZF, MMSE SIC, SD
Tx / Rx Antenna Configuration (Selected Antenna Configuration)	6 x 6 (4 x 4)
Tx / Rx Antenna Distance	10λ / 0.5λ
Channel Coding	Turbo Coding
Mother Code Rate	2/3
HARQ Algorithm	CC, IR, Proposed
Retransmission Code Rate of IR	3/5, 8/15, 1/2, 2/5
Max Retransmission Number	4

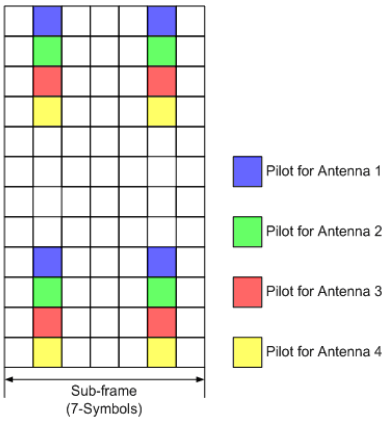

Fig. 8 The structure of the pilot assignment per antenna.

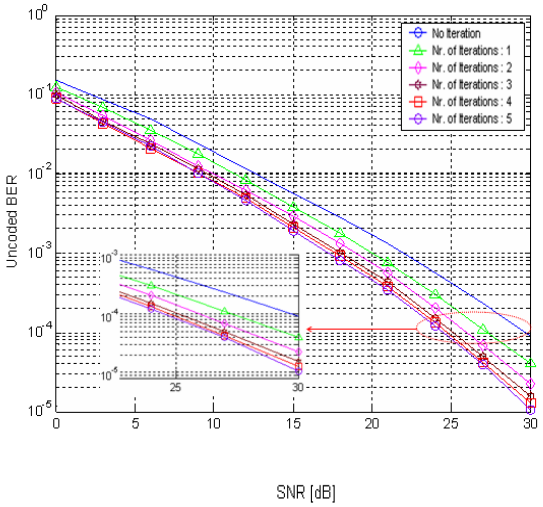

Fig. 9 4 x 4 QPSK uncoded BER performance of the I-BLAST system according to the iteration number.

4.1 Performance of I-BLAST System

Figs. 9 and 10 show the 4 x 4 QPSK uncoded BER and the 4 x 4 16QAM coded BER performance of the I-BLAST system according to the iteration number.

In the case of the uncoded QPSK in Fig. 9, at a target BER of 10^{-4}, SNR improvements by three and five iterations are about 4.8 dB and 5.2 dB, respectively, compared to the case with no iteration. In the case of the coded 16QAM shown in Fig. 10, at a target BER of 10^{-5}, the SNR improvements after three and five iterations are approximately 3 dB and 2.7 dB, respectively, compared to the case with no iteration. From the above results, it can be observed that the detection error, channel estimation error and interference components are nearly eliminated after three iterations. Thus, the ideal number of iterations is determined to be three.

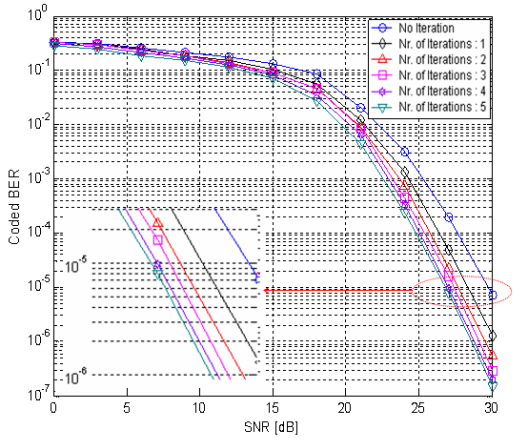

Fig. 10 4 x 4 16QAM coded BER performance of the I-BLAST system according to the iteration number.

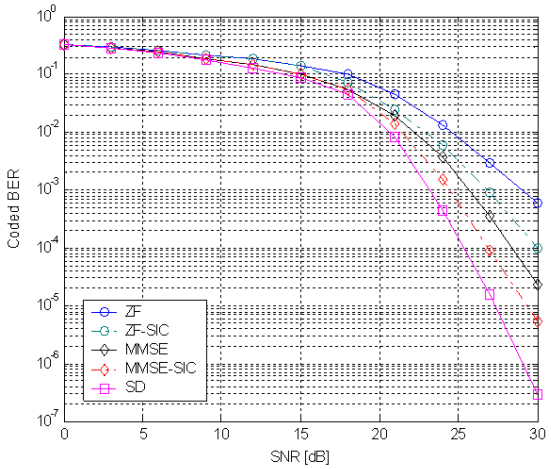

Fig. 11 4 x 4 16QAM coded BER performance of I-BLAST according to MIMO detection methods.

4.2 Performance of MIMO Detectors

The 4 x 4 16QAM coded BER performance of the I-BLAST system is tried with the MIMO detections of the zero forcing (ZF), minimum mean-square error (MMSE), ZF successive interference cancellation (ZF-SIC), MMSE-SIC, and the SD in Fig. 11. It is observed that the SD shows the best performance; the ZF is the simplest but shows the worst performance, as expected. At a target BER of 10^{-5}, the SD gains more than 10 dB of SNR compared to ZF detection. The ZF-SIC and MMSE-SIC schemes are superior to the ZF and MMSE schemes due to the interference cancellation characteristic of SIC among the antennas.

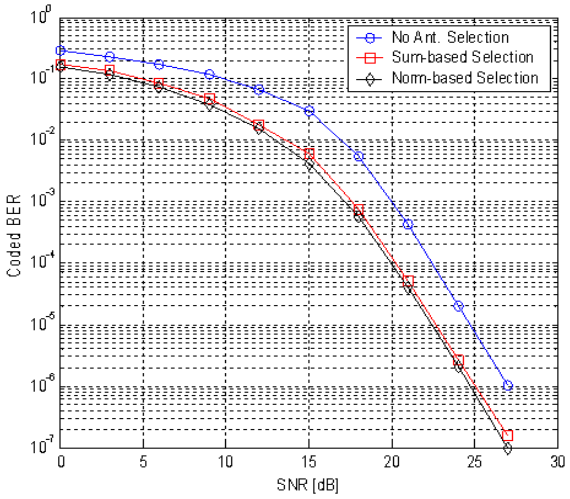

Fig. 12 4 x 4 16QAM coded BER performance of I-BLAST according to antenna selection method.

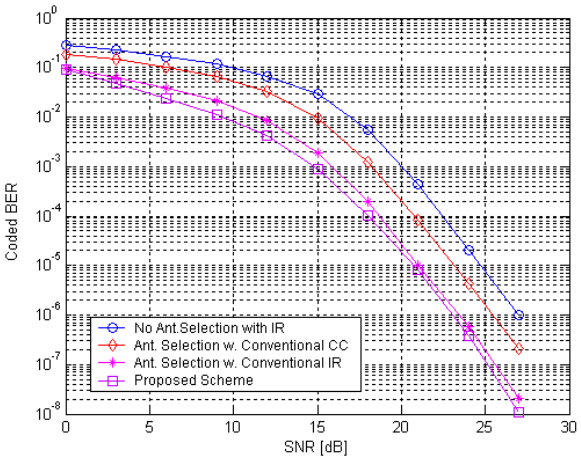

Fig. 13 4 x 4 16QAM coded BER performance of I-BLAST applying HARQ algorithm based on the proposed antenna scheduling.

4.3 Performance of the Proposed MIMO HARQ Algorithm with Antenna Scheduling

In this subsection, the performance of the transmit / receive antenna selection process and the proposed HARQ scheme with antenna scheduling is discussed.

Antenna selection in this subsection is based on the channel sum in Eq. (17) and the channel norm in Eq. (20).

$$\Im_{T_n}^{Norm} = \sum_{m=1}^{n_R} \left\| H_{mn} \right\|^2, \; n = 1, 2 \ldots, n_T$$
$$\Im_{R_m}^{Norm} = \sum_{n=1}^{n_T} \left\| H_{mn} \right\|^2, \; m = 1, 2 \ldots, n_R \qquad (20)$$

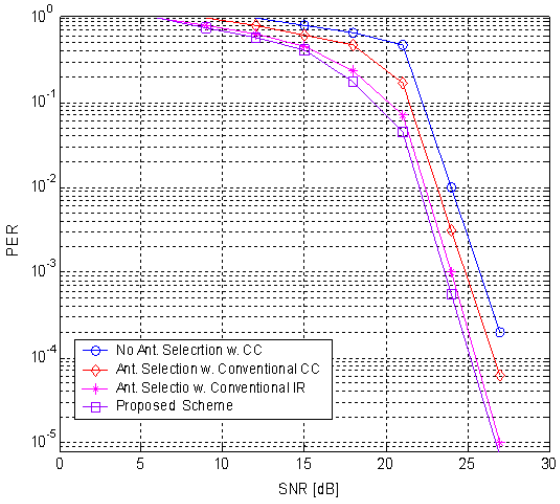

Fig. 14 4 x 4 16QAM PER performance of I-BLAST applying HARQ algorithm based on the proposed antenna scheduling.

Figure 12 shows the 4 x 4 16QAM coded BER performance of the I-BLAST system according to the antenna selection method. The sum-based and norm-based selection methods show nearly identical performances, hence the antenna selection was chosen based on the channel sum due to its simplicity.

Figs. 13 and 14 show the performance of the I-BLAST system with the proposed HARQ algorithm with antenna scheduling. In this simulation, the stop-and-wait (SAW) ARQ scheme is used. The SAW ARQ scheme transmits the packet after receiving ACK or NAK from the receiver, and the new packet is not transmitted during retransmission. In Fig. 13, at the target BER of 10^{-5}, the proposed algorithm is superior to the cases of antenna scheduling with conventional chase combining and with incremental redundancy by the SNR values of 3 dB and 0.5 dB, respectively. In Fig. 14, at the target PER of 10^{-3}, the gain with the two aforementioned schemes by the proposed algorithm becomes 2 dB and 0.7 dB, respectively. This gain by the proposed HARQ algorithm comes from the spatial diversity due to the proposed antenna scheduling.

5. Conclusions

In this paper, the MIMO HARQ algorithm based on the antenna scheduling is proposed. It retransmits a packet using scheduled antennas according to the state of the communication link, as opposed to retransmitting the packet using the same antennas. For the MIMO HARQ system with I-BLAST, the optimal number of iterations is determined, and the performances of detection schemes including sphere decoding are compared. For the proposed antenna scheduling, a channel sum type of antenna selection is adopted considering the tradeoff between performance and complexity. Finally, the proposed MIMO HARQ system based on antenna scheduling is shown to be superior to conventional MIMO HARQ systems due to its spatial diversity gain.

References

[1] M. Sellathurai and S. Haykin, "TURBO-BLAST for wireless communications: Theory and experiments," *IEEE Trans. on Signal Processing*, vol. 50, No. 10, pp. 2538-2546, Oct. 2002.

[2] Marc Engels, *Wireless OFDM Systems.* Kluwer, 2002.

[3] G. L. Stuber, J. Barry, S. McLaughlin, Y. Li, M. A. Ingram, and T. Pratt, "Broadband MIMO-OFDM wireless communications," in *Proc. of IEEE*, vol. 92, Feb. 2004, pp. 271-294.

[4] J. Li and H. Imai, "Performance of hybrid-ARQ protocols with rate compatible turbo codes," in *Proc. Int. Symp. on Turbo Codes*, Sept. 1997, pp. 188-191.

[5] J. M. Shea, "Reliability-based hybrid ARQ," *IEEE Electronics Letters*, vol. 38, pp. 644-645, June 2002.

[6] JinHo Choi, *Adaptive and Iterative Signal Process in Communications*. Cambridge, 2006.

[7] E. Viterbo and J. Boutros, "A universal lattice code decoder for fading channels," *IEEE Trans. on Information Theory*, vol. 45, pp. 1639-1642, July 1999.

[8] A. Wiesel, X. Mestre, A. Pages, and J. R. Fonollosa, "Efficient implementation of sphere demodulation," in *Proc. IEEE Signal Processing Advances in Wireless Comms*., June 2003, pp. 15-18.

[9] D. Wubben, R. Bohnke, J. Rinas, V.Kuhn, and K. D. Kammeyer, "Efficient algorithm for decoding layered space-time codes," *IEEE Electronics Letters,* vol. 37, pp. 1348-1350, Oct. 2001.

[10] 3rd Generation Partnership Project (3GPP) Technical Specification 25.212 Rev. 5.9.0, "Multiplexing and channel coding (FDD)," June 2004.

[11] 3GPP & 3GPP2 Spatial Channel Model AHG, "Spatial channel model text description-Rev 7.0," Aug. 2003.

[12] Motorola, R1-06259, "E-UTRA downlink reference-signal structure, Text Proposal," Jan. 2006.